We have previously reported that CT of the breast is useful for clinical decision making regarding the extent of breast surgery [1–4]. Due to the increase in the number of detector rows in CT scanners, the scan speed and scan range have been increased. However, increasing the number of detector rows does not lead to a significant improvement in the contrast between breast cancer and normal mammary gland tissue. Because CT numbers (Hounsfield Unit) are evaluated in conventional CT scanning, there is no significant difference between 256-row CT and single-slice helical CT in the depiction of the extent of breast cancer. With regard to sensitivity, it remains at 80–90% [1, 3–7]. It is therefore considered necessary to employ image processing techniques, such as the perfusion technique, which permits depiction of blood flow. Perfusion CT results in quantitative visualization of blood flow in parenchymal organs, while maintaining high spatial resolution [8]. By dividing the rate of tissue enhancement by the blood flow, contrast medium is employed as a physiological indicator. The functional images obtained using this technique may provide higher contrast.

The aims of the present study were to apply perfusion techniques to breast tumors using a 256-row MSCT scanner and, using volume perfusion maps generated from the resulting data, evaluate the possibility of precisely depicting the extent of breast cancer—especially in comparison with CT scanning in the early-enhancement phase.

Patients and methods

Subjects

The study protocol was approved by our institutional review board, and written informed consent was obtained from all patients. Due to the limited period of operation of the 256-row MSCT scanner at our institution, seven patients with breast cancer were enrolled in the study between July and September 2006. Their mean age was 62 years (range 44–83 years). Five invasive ductal cancers and two ductal carcinomas in situ were evaluated.

Scan conditions

The CT system employed was a prototype 256-row MSCT scanner (Toshiba Medical Systems Corporation, Tochigi, Japan). The scan conditions were 256 rows × 0.5 mm, 120 kV, 150–250 mA (depending on patient size), 0.5 s/rotation, reconstruction kernel FC13 (standard abdominal reconstruction function), scan field of view (FOV) 400 mm, and display FOV 200 mm. A total of 100 ml of nonionic contrast medium (300 mg I/ml; Omnipaque 300, Daiichi Sankyo Co., Tokyo, Japan) was injected at a rate of 3 ml/s. Intermittent dynamic scanning was performed at 16 time points (before contrast medium injection and at 2, 4, 6.5, 9, 12, 15, 18.5, 22, 26, 30, 34.5, 39, 44, 49, and 54 s after the start of contrast medium injection) during normal respiration, and time–density curves (TDCs) were obtained. No delayed-phase scanning was performed in this study. Simulation analysis was conducted to determine the optimal scan timing.

Generation of perfusion maps

CT images were acquired and transferred to an image processing workstation. The acquired images showed a small amount of displacement due to respiratory motion. Therefore, the image data were shifted in the X–Y–Z planes for each time sequence to perform position-matching.

Perfusion analysis was performed using the maximum slope method. First, a region of interest (ROI) was placed in an artery near the mammary gland tissues, and the maximum CT value (peak arterial enhancement) was measured. The TDCs were then generated for each pixel from time-sequential images, and perfusion values were calculated for all pixels using Eq. 1 [8].

$$\text{Perfusion value} = \frac{\text{maximum rate of tissue enhancement}}{\text{peak arterial enhancement}} \quad (1)$$

The perfusion values were converted to a 256-level color scale to display perfusion maps with a slice thickness of 0.5 mm in the window.

Early-enhancement-phase CT

In conventional CT studies of the breast, scanning is performed 50–60 s after the start of contrast medium injection to depict the early-enhancement phase [1]. Therefore, the CT images acquired at 54 s using the 256-row MSCT scanner were considered to be early-enhancement-phase CT images.

Results

Evaluation based on perfusion values

The TDCs for the main tumors were generated. A steady increase was observed in cases 1–4, and an irregular gradual increase was observed in cases 5–7. The perfusion values for each case are shown in Table 1. The tumors could be distinguished based on the perfusion values in all cases. The perfusion values were 20 or less in normal mammary gland tissue and greater than 40 in tumors, including both the invasive and intraductal components.

Table 1 Perfusion values [ml/min/ml]

Case no.	Pathology	Normal mammary gland	Tumor		
			Invasive component	Intraductal component	LN
1	IDC	5–10	111	NA	150
2	DCIS	1–5	NA	42	
3	IDC with DS	5	95–106	80	
4	IDC with DS	10–20	194	NA	
5	IDC with DS	5	52	37–43	
6	IDC	10	48	NA	
7	DCIS	10–20	NA	140	

DS ductal spread, *NA* not applicable, *LN* lymph node

In general, the perfusion values tended to be slightly lower in the intraductal components than in invasive tumors.

Pathology findings and relationships with CT findings

In three patients with a pathologically demonstrated ductal spread, its extent was clearly depicted in the perfusion map images, parts of which could not be depicted by early-enhancement-phase CT. These images showed good agreement with the pathology findings (Figs. 1, 2, 3). In the four patients with localized tumors, including two with ductal carcinoma in situ, the tumor regions were the same in the perfusion map images, early-phase CT images, and pathology specimens. These results suggest that volume perfusion map imaging using a 256-row MSCT scanner can more precisely depict the extent of the ductal spread than conventional breast CT imaging.

Simulation for reduction of scan time points

The exposure dose was 43.7–45 mSv. To reduce the number of scan time points and the exposure dose, we calculated the variation rate of the TDC gradient to determine the perfusion value. The time points at 4, 6.5, 9.0, and 12.0 s were used as the start points of the TDC gradient, and those at 39.0, 44.0, and 49.0 s were used as the end points. The time point at 0 s was defined as the base value, and the data obtained at these eight points was used to calculate the TDC gradient. The variation rates from the original TDC gradients in each case were 0.7, 2.8, 1.65, 1.5, 2.3, 6.4, and 12.9%, respectively. The variation rates for evaluation of the intraductal component in cases three and four were 2.5 and 3.3%, respectively. The consistency of the graphs in patients showing a steady increase in the TDCs was ensured by performing position matching of the image data. However, in cases 6 and 7, which showed an irregular gradual increase in the TDCs, the variation rates were greater than 6%, which was probably attributable to shifting of the ROIs due to respiratory motion that could not be completely corrected. We speculate that breath-holding may reduce the variation rates, and the results suggest that comparable results could be obtained by performing scanning eight times with breath-holding.

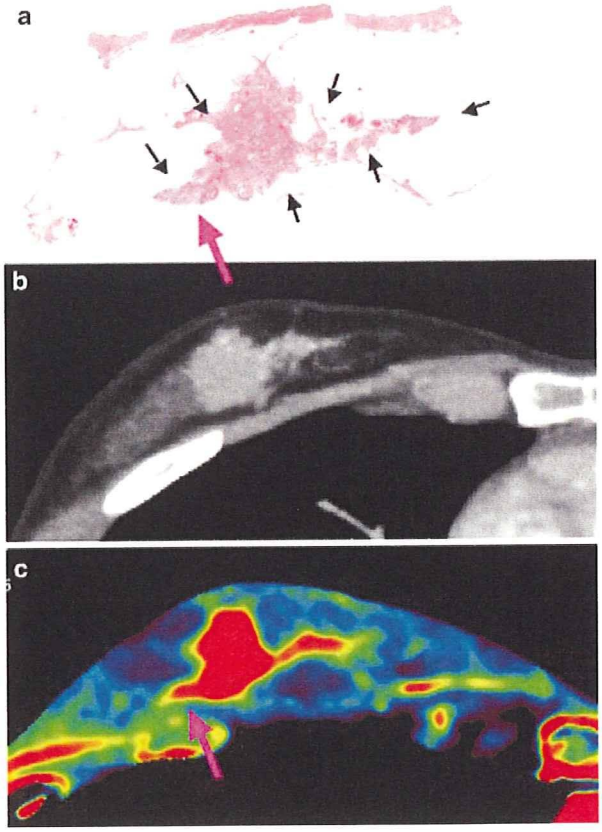

Fig. 1 A 44-year-old woman with invasive ductal carcinoma of the breast. **a** Panoramic view of the tumor in the resected tissues. **b** CT image in the early-enhancement phase. Tumor tissues extending to the left from the main tumor are not depicted. **c** Perfusion map image. The tumor tissues (including the tumor on the left side that could not be visualized in the early-enhancement phase) are clearly depicted (*pink arrow*), showing good agreement with the pathology findings

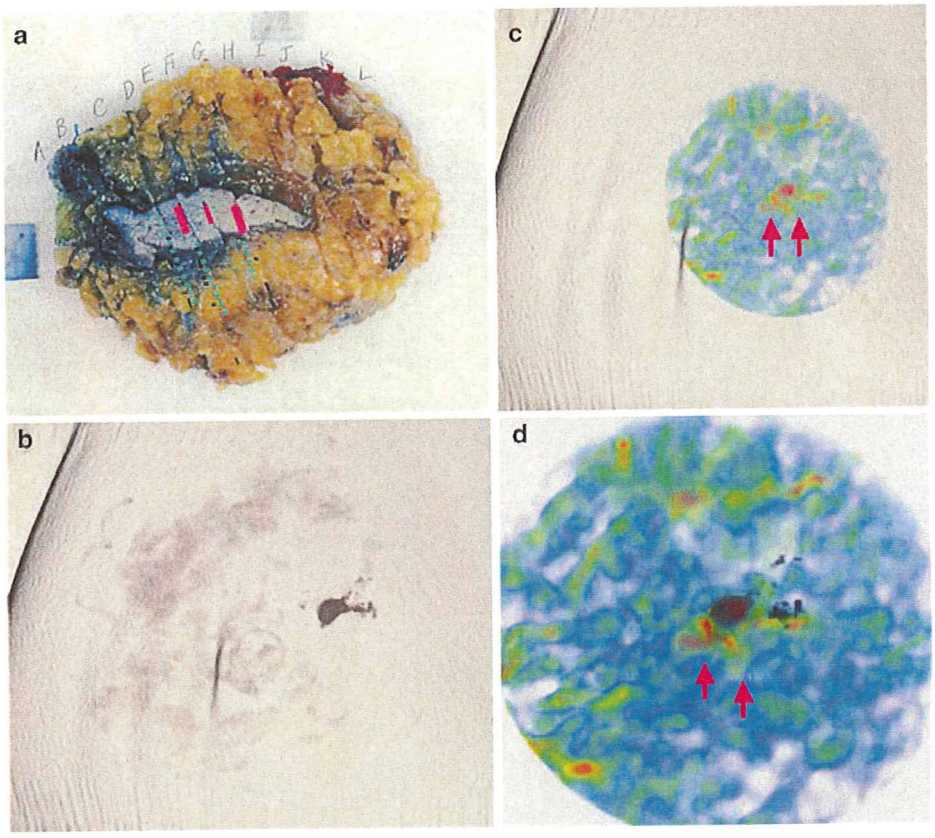

Fig. 2 A 60-year-old woman with invasive ductal carcinoma of the breast. **a** Image showing resected tissues only. *Pink lines* invasive ductal carcinoma. *Green lines* lesion with ductal spread. **b** Three-dimensional CT image in the early-enhancement phase. **c** Perfusion image. **d** Fusion image combining the images shown in **b** and **c**. The lesion with ductal spread located on the side toward the nipple from the main tumor could be depicted only in the perfusion map image (*pink arrows*)

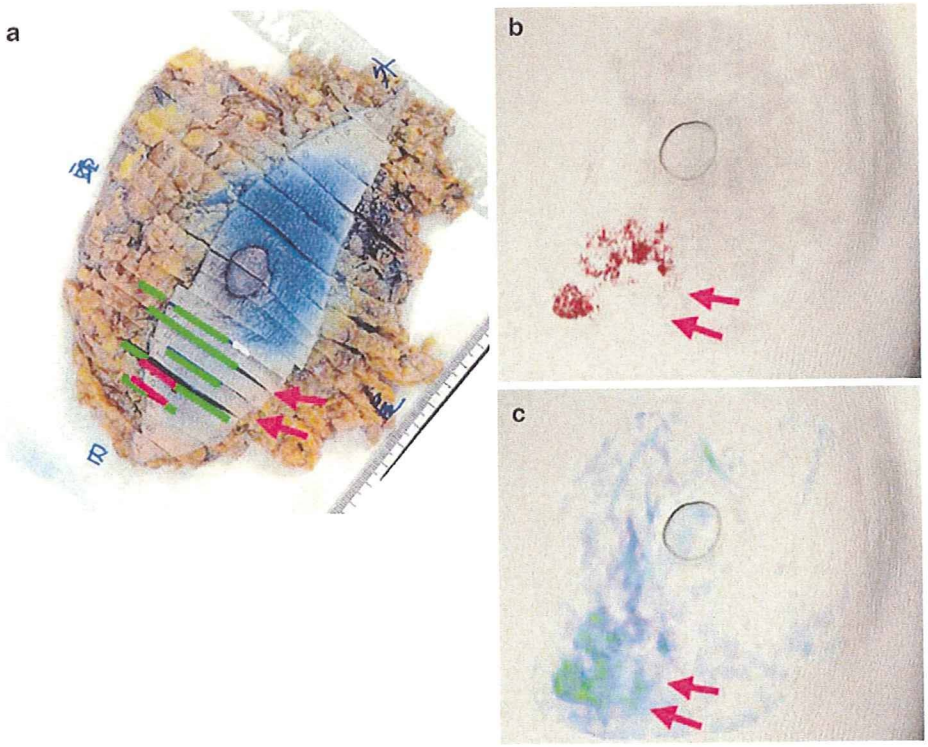

Fig. 3 A 45-year-old woman with invasive ductal carcinoma of the breast. **a** Image showing resected tissues only. *Red lines* tumor invasion. *Green lines* lesion with ductal spread. **b** Three-dimensional CT image in the early-enhancement phase (generated by the volume-rendering method). The intraductal component extending from the main tumor toward the nipple is depicted; the extent of tumor tissue on the right side of the tumor mass is not depicted (*pink arrows*). **c** Perfusion map image. The tumor tissues (including the ductal spread extending to the right of the main tumor that could not be depicted in the early-enhancement phase) are clearly depicted (*pink arrows*), showing good agreement with the pathology findings

Discussion

The results of the present study suggest that perfusion CT can depict the extent of breast cancer more precisely than conventional breast CT in the early-enhancement phase, especially in patients with ductal spread. Perfusion processing was performed for the data acquired by 256-row CT to obtain functional images. As a result, the tissue resolution was increased, making it possible to visualize small lesions, as shown in Figs. 1, 2, and 3. One reason for being able to visualize such small lesions was the integration effect of aggregate time. Then the total amount of information became big. These findings suggest that CT images can be improved not only in terms of spatial resolution by employing a larger number of detector rows, but also in terms of contrast levels by performing image processing, which may lead to higher sensitivity.

Precisely determining the extent of primary breast cancer before surgery is essential for achieving local control and an acceptable cosmetic result [9–11]. While breast MRI is known to be useful for assessing the extent of cancer, it requires both a dedicated breast coil and radiologists who are experts in breast imaging and familiar with the optimal imaging sequences and other technical details related to image interpretation [12]. Moreover, the shape of the breast in MRI images obtained in the prone position differs from that in the supine position during surgery. Breast CT images acquired in the supine position therefore provide more accurate information for surgical planning [1, 9]. Some studies have reported that MSCT images can be used to assess the extent of breast cancer with a high degree of accuracy [5–7, 13]. In another study, CT and MRI examinations were performed to assess the extent of cancer in the same patient, and the results showed that the MR images were superior or equal to the CT images in terms of sensitivity, that the CT images were superior in terms of specificity, and that the MR images and the CT images were equal in terms of diagnostic accuracy [14–16]. Recent improvements in MRI systems have led to an increase in the specificity of MRI images. Determining whether CT perfusion maps are superior to MR images for evaluating the extent of cancer is a subject for future research.

Only one recent report has described the usefulness of perfusion CT in patients with breast cancer [17]. The patients were examined using a 16-row MSCT scanner, and perfusion maps were obtained over a range of 8 mm. That study suggested the feasibility of breast cancer perfusion and reported differences in the perfusion values among histological subtypes.

One disadvantage of breast CT is radiation exposure. Scanning with the 256-row MSCT scanner was performed in patients at 16 time points from 0 to 54 s at 43.7–45 mSv. Simulation analysis suggested that the exposure dose could be reduced by half (to 20 mSv) if scanning were performed eight times with breath-holding. In addition, it is thought that the linear high-perfusion areas observed at the borders represented artifacts due to respiratory motion. It is therefore expected that clearer images could be obtained with breath-holding. At time points of 12.0 s or earlier and at 39.0 s or later, which were used in the simulation, if scanning were performed with breath-holding in the inspiratory phase, it might be possible to reduce the fluctuation in TDCs, permitting perfusion maps of equivalent level to be generated and images with fewer artifacts to be obtained. In the future, it should become possible to obtain clearer images with reduced exposure dose by taking these scan conditions into consideration.

This pilot study with 256-row MSCT is the world's first trial. We synchronized the timing for scan, injection speed, and perfusion analysis algorithm (maximum slope method), all of which have been used for liver cases. It remains a matter of discussion whether to evaluate an optimum model for outflow of contrast medium, injection speed, and scan timing.

Conclusion

The results of this pilot study suggest that volume perfusion images (as functional images) acquired using 256-row CT may be useful for depicting, with higher sensitivity, the extent of breast cancer. Further research is needed to validate these results.

Acknowledgments This work was supported in part by Health and Labour Sciences Research Grants for Third Term Comprehensive Control Research for Cancer.

References

1. Akashi-Tanaka S, Fukutomi T, Miyakawa K, Uchiyama N, Tsuda H. Diagnostic value of contrast-enhanced computed tomography for diagnosing the intraductal component of breast cancer. Breast Cancer Res Treat. 1998; 49:79–86.
2. Akashi-Tanaka S, Fukutomi T, Miyakawa K, Tsuda H. Diagnostic value of enhanced computed tomography in the detection of the widely spreading intraductal component of breast cancer: case reports. Breast Cancer. 1997; 4(1):29–32.
3. Akashi-Tanaka S, Fukutomi T, Miyakawa K, Nanasawa T, Matsuo K, Hasegawa T, et al. Contrast-enhanced computed tomography for diagnosing the intraductal component and small invasive foci of breast cancer. Breast Cancer. 2001; 8(1):10–15.
4. Akashi-Tanaka S, Fukutomi T, Sato N, Miyakawa K. The role of computed tomography in the selection of breast cancer treatment. Breast Cancer. 2003; 10(3):198–203.
5. Fujita T, Doihara H, Takabatake D, Takahashi H, Yoshitomi S, Ishibe Y, et al. Multidetector row computed tomography for diagnosing intraductal extension of breast carcinoma. J Surg Oncol. 2005; 91:10–6.

6. Uematsu T, Sano M, Homma K, Shiina M, Kobayashi S. Three-dimensional helical CT of the breast: accuracy for measuring extent of breast cancer candidates for breast conserving surgery. Breast Cancer Res Treat. 2001; 65:249–57.
7. Takase K, Furuta A, Harada N, Harada N, Takahashi T, Igarashi K, et al. Assessing the extent of breast cancer using multidetector row helical computed tomography. J Comput Assist Tomogr. 2006; 30:479–85.
8. Miles K. Measurement of tissue perfusion by dynamic computed tomography. Br J Radiol. 1991; 64:409–12.
9. Uematsu T, Sano M, Homma K, Sato N. Value of three-dimensional helical CT image-guided planning for made-to-order lumpectomy in breast cancer patients. Breast J. 2004; 10(1):33–7.
10. Esserman L, Hylton N, Yassa L, Barclay J, Frankel S, Sickles E. Utility of magnetic resonance imaging in the management of breast cancer: evidence for improved preoperative staging. J Clin Oncol. 1999; 17(1):110–9.
11. Newman LA, Kuerer HM. Advances in breast conserving therapy. J Clin Oncol. 2005; 23:1685–97.
12. NCCN Breast cancer panel members. Principles of dedicated breast MRI testing. NCCN Practice Guidelines in Oncology. vol. 2. 2008:30.
13. Inoue T, Tamaki Y, Hamada S, Yamamoto S, Sato Y, Tamura S, et al. Usefulness of three-dimensional multidetector-row CT images for preoperative evaluation of tumor extension in primary breast cancer patients. Breast Cancer Res Treat. 2005; 89(2):119–25.
14. Nakahara H, Namba K, Wakamatsu H, Watanabe R, Furusawa H, Shirouzu H, et al. Extension of breast cancer: comparison of CT and MRI. Radiat Med. 2002; 20(1):17–23.
15. Tozaki M, Uno H, Kobayashi T, Aiba K, Yoshida K, Takeyama H, et al. Histologic breast cancer extent after neoadjuvant chemotherapy: comparison with multidetector-row CT and dynamic MRI. Radiat Med. 2004; 22(4):246–53.
16. Shimauchi A, Yamada T, Sato A, Takase K, Usami S, Ishida T, et al. Comparison of MDCT and MRI for evaluating the intraductal component of breast cancer. Am J Roentgenol. 2006; 187(2):322–9.
17. Hirasawa H, Tsushima Y, Hirasawa S, Takei H, Taketomi-Takahashi A, Takano A, et al. Perfusion CT of breast carcinoma: arterial perfusion of nonscirrhous carcinoma was higher than that of scirrhous carcinoma. Acad Radiol. 2007; 14(5):547–52.

Jpn J Clin Oncol 2009;39(2)132

Image of the Month

A Case of Ductal Carcinoma In Situ of the Breast

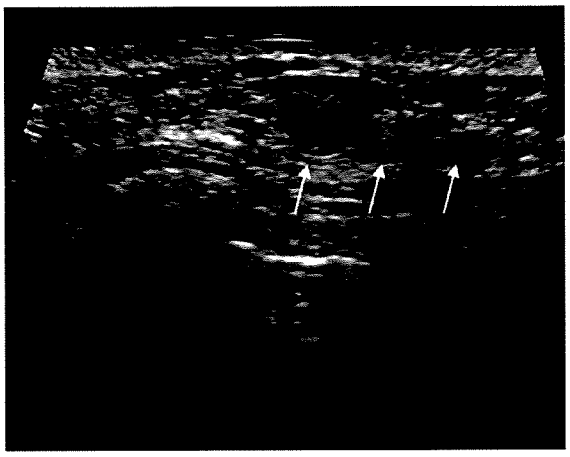

Figure 1.

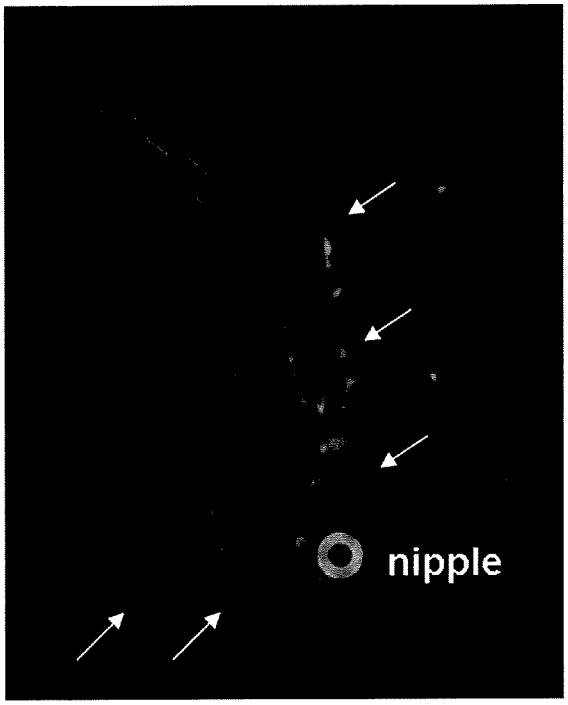

Figure 2.

A 55-year-old woman underwent a follow-up study 3 years after left mastectomy for ductal carcinoma *in situ* (DCIS). On ultrasonography (US), a line of small hypoechoic areas was found in the right breast (Fig. 1), which was not shown on mammography. On magnetic resonance imaging (MRI), an irregularly enhanced segmental tumor with a maximum length of 7 cm was demonstrated in the right upper outer quadrant (Fig. 2). Vacuum-assisted core biopsy of the tumor under US-guidance revealed DCIS. She underwent right mastectomy with sentinel node biopsy. The sentinel nodes were negative for cancer. The histopathological extension of the tumor was more precisely predicted on MRI than on US.

In review of 137 patients with DCIS, we also found that the histopathological extension of the tumor was more precisely predicted on MRI than on mammography or US. Although microcalcification on mammography is considered a key finding for detecting DCIS, MRI might be an essential imaging study for patients with DCIS.

Miwa Yoshida and Takayuki Kinoshita
Breast Surgery Division
National Cancer Center Hospital
Tokyo, Japan
doi:10.1093/jjco/hyn152

Breast Cancer (2009) 16:68–71
DOI 10.1007/s12282-008-0057-9

CASE REPORT

Primary small cell carcinoma of the breast

Takashi Hojo · Takayuki Kinoshita · Tadahiko Shien · Kotoe Terada · Shigemichi Hirose · You Isobe · Shunji Ikeuchi · Kiyoshi Kubochi · Sumio Matsumoto · Akashi-Tanaka Sadako

Received: 19 December 2006 / Accepted: 3 March 2008 / Published online: 27 May 2008

Abstract Primary small cell carcinoma of the breast is a very rare disease, and only a few case reports have described small cell carcinoma of the breast that responds to chemotherapy. Here, we report a case of primary small cell carcinoma of the breast that was treated with surgery and chemotherapy for postoperative local recurrence in the chest wall and metastasis to the liver. The metastatic lesions showed a partial response (PR) to carboplatin and irinotecan, but did not respond to subsequent Taxotere and doxifluridine (5′-DFUR) treatment. We then treated the metastatic lesions with CBDCA and etoposide (VP-16), and were able to stop disease progression. Small cell carcinoma of the breast is as aggressive as its pulmonary counterpart. Therefore, the best therapy for primary small cell carcinoma of the breast may be surgery followed by adjuvant therapy similar to that recommended for small cell lung carcinoma.

Keywords Breast · Small cell carcinoma · Chemotherapy

T. Hojo (✉) · T. Kinoshita · T. Shien · K. Terada · A.-T. Sadako
Breast Surgery Division, National Cancer Center Hospital, 5-1-1 Tsukiji, Chuo-ku, Tokyo 104-0045, Japan
e-mail: tahojo@ncc.go.jp

S. Hirose
Pathology Division, National Hospital Organization Tokyo Medical Center, 2-5-1 Higashigaoka, Meguro-ku, Tokyo 152-8902, Japan

Y. Isobe · S. Ikeuchi · K. Kubochi · S. Matsumoto
Surgery Division, National Hospital Organization Tokyo Medical Center, 2-5-1 Higashigaoka, Meguro-ku, Tokyo 152-8902, Japan

Introduction

Primary small cell carcinoma of the breast is a very rare disease, with fewer than 33 cases described in the literature [1–15, 27–29]. There are even fewer reports of this disease responding to chemotherapy [1, 3, 7–13, 15]. We report here a case in which a hepatic metastasis of primary breast small cell carcinoma showed a response to chemotherapy. We discuss treatment strategies for primary breast small cell carcinoma based on this case and previous reports.

Case report

A 60-year-old, post-menopausal Japanese woman presented at the hospital with a mass in her right breast that she had noticed 3 months earlier. Physical examination revealed a 2.2 × 1.5-cm firm non-tender tumor with irregular borders in the upper-outer quadrant of the right breast; the nipple-tumor distance was 5.5 cm. There was no nipple discharge, and bilateral axillary lymph nodes showed no abnormality. Laboratory data and tumor markers were within normal ranges [carcinoembryonic antigen (CEA), carbohydrate antigen 15-3 (CA15-3), and National Cancer Center-Stomach-439 (NCC-ST-439)]. A mammogram of the right breast showed a microlobulated mass without calcification. An ultrasonogram confirmed the heterogeneity of the mass and showed no intraductal component. MRI showed a distinctly contrasting mass of about 3.0 × 2.0 cm in the upper-outer quadrant of the right breast, and neither ductal spread nor multiple lesions were observed. Furthermore, a computed tomography scan revealed no obvious findings of lung tumors or distant organ metastasis. We diagnosed the mass as cancer by

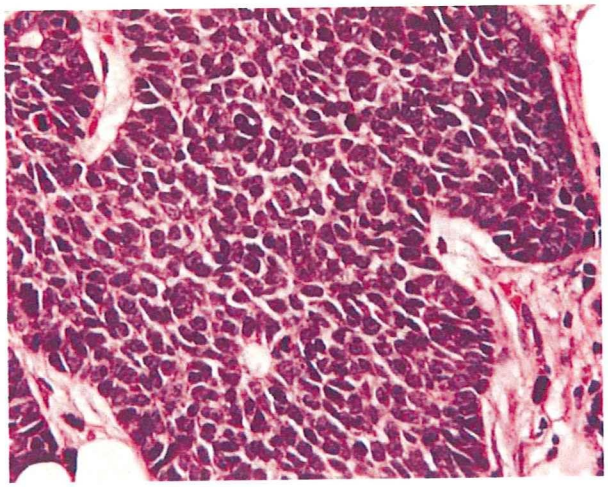

Fig. 1 Pathological findings (hematoxylin-eosin). Histopathological examination by hematoxylin and eosin staining showed that the neoplastic cells have scant cytoplasm and hyperchromatic nuclei. Some rosette-like structures are present in this nest

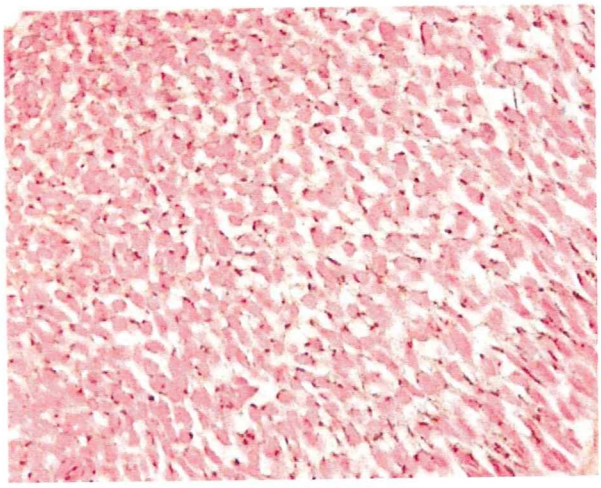

Fig. 2 Pathological findings (immunohistochemical staining for Grimelius). Grimelius staining was positive for narrow cytoplasm of neoplastic cells

needle biopsy. The breast cancer was preoperatively classified as T2N0M0 (UICC, 6th edition, 2002).

We planned conservation surgery with axillary lymph node dissection. However, this was changed to modified radical mastectomy because the margin of the removed specimen showed cancer invasion. The tumor was a solid yellow-white mass of 3.0 × 1.0 cm in the greatest cut dimension, and the margin was infiltrating with an indistinct border. No axillary lymph node involvement was observed.

Histopathological examination by hematoxylin and eosin staining showed that the tumor was composed of nests of small cells with round to fusiform shape, scant cytoplasm, finely granular nuclear chromatin and absent or inconspicuous nucleoli. Occasionally, rosette-like structures were observed. Foci in the ductal components were Pagetoid spread (Fig. 1). The results of immunostaining were as follows. The tumor cells were positive for Grimelius, cytokeratinAE1/AE3, neuron-specific enolase (NSE), CD56, bcl-2 and CD117 (c-kit), but were negative for Chromogranin, cytokeratin34BE12, synaptophysin, estrogen receptor, progesterone receptor and Her2/neu. The patient did not undergo adjuvant therapy.

A mass later appeared on the chest wall at the operative site. This was diagnosed as breast small cell carcinoma by cytodiagnosis. Multiple metastases were found on the liver by abdominal computed tomography, but no metastases were found in other organs. Chemotherapy was performed using a regimen for pulmonary small cell carcinoma: day 1 cisplatin at 60 mg/m^2 and days 1, 8 and 15 CPT-11 at 60 mg/m^2. However, we changed cisplatin to carboplatin, because the patient experienced grade 2 neutropenia, grade 2 leucopenia and grade 2 vomiting (NCI-CTC) following the first administration. The patient was treated with carboplatin (300 mg/m^2) on day 1 and CPT-11 (60 mg/m^2) on days 1, 8 and 15 every 3 weeks for five cycles. The patient experienced no grave side effects. The local recurrence disappeared during chemotherapy, and the metastatic lesions on the liver were reduced by 71% (Fig. 2). The second course of chemotherapy administered docetaxel (DTX) and 5′-DFUR; however, the hepatic tumors progressed during this course. The second course is a regimen often used to treat breast cancer and other regional carcinomas; however, this therapy was not efficacious in this case (Fig. 3). Therefore, we treated with a regimen of carboplatin (300 mg/m^2) on day 1 and etoposide (80 mg/m^2) on days 1 and 2 every 3 weeks for four cycles. The metastatic lesions on the liver were reduced by 5.8% during the third course of treatment (Fig. 3). Subsequently, the liver metastasis progressed, but the patient chose to stop chemotherapy. The patient passed away 26 months following the initial surgery.

Discussion

Herein, we report treatment of a primary small cell carcinoma of the breast.

The tumor was positive for Grimelius (Fig. 3), but negative for Chromogranin by immunostaining. Because the Grimelius staining was weak, we thought it was possible that the tumor was a small cell carcinoma of low secretory ability; this would also explain the lack of Chromogranin staining.

Extrapulmonary small cell carcinoma (EPSCC), a rare neoplasm, has been increasingly recognized as a clinicopathologic entity distinct from small cell carcinoma of the

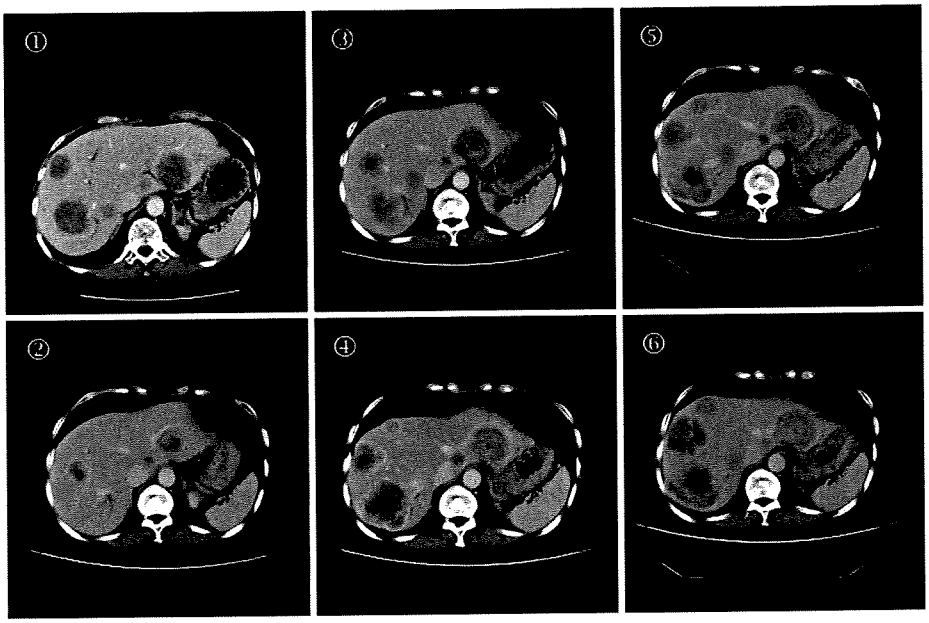

Fig. 3 Computed tomography (CT). Use of chemotherapy for hepatic metastasis and evaluation by CT. The patient was treated with a combination of carboplatin and CPT 11 for (1) to (2) period, and a partial response was achieved. The patient was treated with docetaxel and 5′-DFUR in periods (3) to (4), and progressive disease was observed. Carboplatin and VP-16 treatment was administered in periods (5) to (6), resulting in stable disease

Table 1 Reported cases of primary mammary small cell carcinoma: clinical summary

Authors	Neo-adjuvant (regimen)	Adjuvant (regimen)	Chemotherapy for MBC (regimen)	Response	Location of MBC	Follow-up (month)	Status
Stein et al. [13]	CDDP + VP16	ND		NC		24	Alive
Mariscal et al. [7]	CDDP + VP16	ND		CR		6	Alive
Samli et al. [9]	CEF	ND		Response		6	Alive
Sebenik et al. [10]	CDDP + VP16	CDDP + VP16		CR		33	Alive
Adegbola et al. [1]		CDDP + VP16				48	Alive
		CDDP + VP16				20	Died
		CDDP + VP16				6	Alive
Sridhar et al. [12]		AD + CDDP				18	Alive
Wade et al. [14]		AC + VCR				9	Died
Yamasaki et al. [15]		CMF				16	Alive
Papotti et al. [8]		TAM				44	Alive
		TAM				9	Alive
		ND	CMF	PD	HEP/BRA	14	Died
Francois et al. [3]		ND	AC + VP16	PR	LYM/PUL	21	Died
Kitakata et al. [27]		EC + DTX				22	Alive
Present case		ND	CBDCA + CPT11	PR	SKI/HEP	26	Died

ND not done, *MBC* metastatic breast cancer, *CDDP* cisplatin, *AD* adriamycin, *VCR* vincristine, *CBDCA* carboplatin, *CPT-11* irinotecan, *CMF* cyclophosphamide, methotrexate and fluorouracyl, *EC* epirubicin and cyclophosphamide, *DTX* docetaxel, *TAM* tamoxifen, *HEP* hepatic, *BRA* brain, *LYM* lymph nodes, *PUL* pulmonary, *SKI* skin

lung. It has been estimated that approximately 1,000 new cases of extrapulmonary small cell carcinoma are diagnosed annually in the US, with an overall incidence of 0.1–0.4% [17]. Approximately 2.5% of all small cell cancers occur in extrapulmonary sites [18]. Irfan [19] reported that the gastrointestinal system (45%), urinary bladder (27%) and uterus (9%) are the most common extrapulmonary sites of small cell carcinoma. There is no standard treatment for limited extrapulmonary small cell carcinoma. In recent years, surgery, if undertaken, was usually performed after induction chemotherapy. Chemotherapy for EPSCC usually follows regimens used to treat small cell lung carcinoma. Cisplatin, etoposide, cyclophosphamide and doxorubicin represent the backbone of most of the combinations used. The overall response rate in extensive disease, using cisplatin-based or cyclophosphamide/doxorubicin

with vincristine or etoposide chemotherapy, is 70–90% [17, 20–26].

Treatment for breast cancer typically involves both local and systemic treatment; however, as small cell carcinoma of the breast is extremely rare, treatment has not been established. In this case, chemotherapeutic regimens typically used to treat small cell lung carcinoma were effective against the breast small cell carcinoma.

In the literature, we were able to identify four reports of neo-adjuvant chemotherapy [7, 10, 13], ten reports of adjuvant therapy [1, 8, 10, 12, 14, 15, 27] and three reports of therapy for metastasis of breast small cell carcinoma [3, 8].

In three of the four neo-adjuvant cases, chemotherapy regimens for small cell lung carcinoma were used. In two of these cases, a complete response was observed.

In five of the ten adjuvant cases, chemotherapy regimens for small cell lung carcinoma were used, and in three of these cases, the patient survived.

Taken together, these cases suggest that chemotherapeutic regimens typically used to treat small lung cell carcinoma can be effective against small cell carcinoma of the breast (Table 1). The best treatment for primary small cell carcinoma of the breast may therefore be surgery followed by such chemotherapeutic regimens.

References

1. Adegbola T, Connolly CE, Mortimer G. Small cell neuroendocrine carcinoma of the breast: a report of three cases and review of the literature. J Clin Pathol. 2005;58:775–8.
2. Bigotti G, Coli A, Butti A, del Vecchio M, Tartaglione R, Massi G. Primary small cell neuroendocrine carcinoma of the breast. J Exp Clin Cancer Res. 2004;23:691–6.
3. Francois A, Chatikhine VA, Chevallier B, Ren GS, Berry M, Chevrier A, Delpech B. Neuroendocrine primary small cell carcinoma of the breast. Report of a case and review of the literature. Am J Clin Oncol. 1995;18:133–8.
4. Fukunaga M, Ushigome S. Small cell (oat cell) carcinoma of the breast. Pathol Int. 1998;48:744–8.
5. Hoang MP, Maitra A, Gazdar AF, Albores-Saavedra J. Primary mammary small-cell carcinoma: a molecular analysis of 2 cases. Hum Pathol. 2001;32:753–7.
6. Jundt G, Schulz A, Heitz PU, Osborn M. Small cell neuroendocrine (oat cell) carcinoma of the male breast. Immunocytochemical and ultrastructural investigations. Virchows Arch A Pathol Anat Histopathol. 1984;404:213–21.
7. Mariscal A, Balliu E, Diaz R, Casas JD, Gallart AM. Primary oat cell carcinoma of the breast: imaging features. AJR Am J Roentgenol. 2004;183:1169–71.
8. Papotti M, Gherardi G, Eusebi V, Pagani A, Bussolati G. Primary oat cell (neuroendocrine) carcinoma of the breast. Report of four cases. Virchows Arch A Pathol Anat Histopathol. 1992; 420:103–8.
9. Samli B, Celik S, Evrensel T, Orhan B, Tasdelen I. Primary neuroendocrine small cell carcinoma of the breast. Arch Pathol Lab Med. 2000;124:296–8.
10. Sebenik M, Nair SG, Hamati HF. Primary small cell anaplastic carcinoma of the breast diagnosed by fine needle aspiration cytology: a case report. Acta Cytol. 1998;42:1199–203.
11. Shin SJ, DeLellis RA, Ying L, Rosen PP. Small cell carcinoma of the breast: a clinicopathologic and immunohistochemical study of nine patients. Am J Surg Pathol. 2000;24:1231–38.
12. Sridhar P, Matey P, Aluwihare N. Primary carcinoma of breast with small-cell differentiation. Breast. 2004;13:149–51.
13. Stein ME, Gershuny A, Abdach L, Quigley MM. Primary small-cell carcinoma of the breast. Clin Oncol (R Coll Radiol). 2005;17:201–2.
14. Wade PM Jr, Mills SE, Read M, Cloud W, Lambert MJ 3rd, Smith RE. Small cell neuroendocrine (oat cell) carcinoma of the breast. Cancer. 1983;52:121–5.
15. Yamasaki T, Shimazaki H, Aida S, Tamai S, Tamaki K, Hiraide H, Mochizuki H, Matsubara O. Primary small cell (oat cell) carcinoma of the breast: report of a case and review of the literature. Pathol Int. 2000;50:914–8.
16. Fitzgibbons PL, Page DL, Weaver D, Thor AD, Allred DC, Clark GM, Ruby SG, O'Malley F, Simpson JF, Connolly JL, et al. Prognostic factors in breast cancer. College of American pathologists consensus statement 1999. Arch Pathol Lab Med. 2000;124:966–78.
17. Remick SC, Hafez GR,Carbone PP. Extrapulmonary small cell carcinoma: a review of the literature with emphasis on therapy and outcome. Medicine. 1987;66:457–71.
18. Remick SC, Ruckdeschel JC. Extrapulmonary and pulmonary small cell carcinoma: tumor biology, therapy, and outcome. Med Pediatr Oncol. 1992;20:89–99.
19. Irfan C, Hakan K, Sernaz U, Kazim U, Ufuk U, Zafer K, Murat C, Mert S, Fusun T, Cem U. Extrapulmonary small-cell carcinoma compared with small-cell lung carcinoma. Am Cancer Soc. 2007;110:1068–76.
20. Brenner B, Tang LH, Klimstra DS. Small-cell carcinoma of the gastrointestinal tract: a review. J Clin Oncol. 2004;22:2730–9.
21. Galanis E, Frytak S, Lloyd RV. Extrapulmonary small cell carcinoma. Cancer. 1997;79:1729–36.
22. Kim JH, Lee SH, Park J, et al. Extrapulmonary small-cell carcinoma: a single-institution experience. Jpn J Clin Oncol. 2004;34:250–4.
23. Haider K, Shahid RK, Finch D, et al. Extrapulmonary small cell cancer: a Canadian province's experience. Cancer. 2006; 107:2262–9.
24. Sengoz M, Abacioglu U, Salepci T, et al. Extrapulmonary small cell carcinoma: multimodality treatment results. Tumori. 2003; 89:274–7.
25. Kurt E, Sezgin C, Evrensel T, et al. Therapy, outcome and analysis of c-kit expression in patients with extrapulmonary small cell carcinoma. Int J Clin Pract. 2005;59:537–43.
26. Van Der Gaast A, Verwey J, Prins E, et al. Chemotherapy as treatment of choice in extrapulmonary undifferentiated small cell carcinomas. Cancer. 1990;65:422–44.
27. Hidekazu K, Kazuo Y, Hiroshi M, Yutaka T. A case of primary small cell carcinoma of the breast. Breast Cancer. 2007;14:414–9.
28. Wenyong Z, Syed AH. Mammary small-cell carcinoma with dimorphic phenotype. The Breast J. 2007;13:529–30.
29. Shaco-Levy R, Dyomin V, Kachko L, Sion-Vardy N, Geffen DB, Koretz M. Small-cell carcinoma of the breast: case report. Eur J Gynaecol Oncol. 2007;28:142–4.

Breast Cancer (2009) 16:30–36
DOI 10.1007/s12282-008-0044-1

ORIGINAL ARTICLE

Usefulness of preoperative multidetector-row computed tomography in evaluating the extent of invasive lobular carcinoma in patients with or without neoadjuvant chemotherapy

Tadahiko Shien · Sadako Akashi-Tanaka · Miwa Yoshida · Takashi Hojo · Eriko Iwamoto · Kunihisa Miyagawa · Takayuki Kinoshita

Received: 22 August 2007 / Accepted: 21 January 2008 / Published online: 25 March 2008

Abstract
Background The present study was conducted to assess the clinical usefulness of multidetector-row CT (MDCT) in determining the extent of invasive lobular carcinoma (ILC) and especially the extent of residual tumor after neoadjuvant chemotherapy (NAC).
Patients and methods The subjects were 24 patients with primary ILC who underwent surgery without NAC and 17 patients with ILC who underwent surgery after NAC at National Cancer Center Hospital (NCCH) between April 1999 and December 2005. The extent of primary ILC was assessed by ultrasound, mammography, and MDCT before surgery, and the results obtained using each modality were compared with the results of pathological examination after surgery. In addition, the characteristic findings of ILC obtained by MDCT were assessed. Similarly, the extent of residual tumor after NAC was evaluated using ultrasound, mammography, and MDCT before surgery in the subjects who underwent NAC, and the results obtained by each modality were compared with the results of pathological examination after surgery.
Results The findings of primary ILC obtained by MDCT showed that the carcinoma was the non-localized type rather than the localized type in 63% of the subjects. In addition, with regard to the pattern of time-sequential contrast enhancement, the persistent pattern (in which tumor enhancement is strong in the late phase rather than in the early phase) was observed in 46% of the subjects, and the plateau pattern (in which contrast enhancement is weak in both the early phase and the late phase) was observed in 38% of the subjects. These trends were significant in the subjects who underwent NAC and in whom tumor enhancement could not be clearly observed by MDCT. Assessment of the extent of carcinoma showed that the diagnostic accuracy of MDCT was 79%, as compared with 71% for either ultrasound or mammography. Assessment of the extent of carcinoma after NAC also showed that the diagnostic accuracy of MDCT was 71%, as compared with 48% for ultrasound and 53% for mammography, indicating that MDCT provided the highest accuracy. It should be noted that for all modalities, the extent of ILC was not overestimated as compared with the tumor diameter measured during pathological examination.
Conclusion Assessment by MDCT showed that ILC tends to be diffuse, tumor enhancement tends to be very weak, and the rate of enhancement tends to be low. In addition, MDCT was found to be useful for determining the extent of carcinoma, and the diagnostic accuracy of MDCT, especially in determining the extent of carcinoma after NAC, was much higher than that of ultrasound or mammography.

Keywords Breast · MDCT · Invasive lobular carcinoma · Neoadjuvant chemotherapy

Abbreviations

MDCT	Multidetector-row computed tomography
NAC	Neoadjuvant chemotherapy
ILC	Invasive lobular carcinoma

T. Shien (✉) · S. Akashi-Tanaka · M. Yoshida · T. Hojo · T. Kinoshita
Division of Breast Surgery, National Cancer Center Hospital, 1-1-5 Tsukiji, Chuo-ku, Tokyo 104-0045, Japan
e-mail: tshien@ncc.go.jp

E. Iwamoto · K. Miyagawa
Department of Diagnostic Radiology, National Cancer Center Hospital, 1-1-5 Tsukiji, Chuo-ku, Tokyo 104-0045, Japan

Introduction

Although invasive lobular carcinoma (ILC) accounts for 10 to 15% of all breast cancers in the USA, it is considered to be relatively rare in Japan. However, the frequency of ILC has recently been increasing, and ILC is therefore becoming a focus of interest. Because ILC extends over a wide range as compared with invasive intraductal carcinoma and because multicentric carcinoma is observed in some cases, it is difficult to determine the extent of breast cancer before surgery [1–5]. Nevertheless, evaluating the extent of breast cancer is very important for determining whether or not breast-conserving therapy is indicated. Recently, neoadjuvant chemotherapy (NAC) has been employed before surgery for the treatment of not only regional advanced breast cancer, but also breast cancer in which the tumor diameter is relatively small. The primary objective of NAC is to minimize the amount of breast tissue that needs to be resected by reducing the size of the tumor, permitting breast-conserving therapy to be employed in a larger number of cases. It is, therefore, considered that precisely determining the extent of residual tumor before surgery is of the utmost importance. However, it is very difficult to determine the extent of residual tumor after NAC as compared with primary breast cancer, and various studies are currently being conducted to identify the most suitable modality for determining the extent of residual tumor [6–15]. In the present retrospective study, cases in which contrast multidetector-row CT (MDCT) was used to examine ILC before surgery were evaluated, and the usefulness of preoperative MDCT in determining the extent of ILC with or without NAC was assessed by comparing the results of MDCT, the results of ultrasound and mammography, and the findings of pathological examination after surgery.

Patients and methods

Patients

The study group included 24 women with operable ILC and 17 women with operable ILC who received NAC at the National Cancer Center Hospital (NCCH) in Tokyo between April 1999 and December 2005. Tumor size was evaluated before surgery by contrast-enhanced computed tomography (CE-CT), ultrasound, and mammography.

The surgical treatment employed was mastectomy or breast-conserving surgery with axillary lymph node dissection and that was decided from both of preoperative general diagnosis (palpation, MMG, US and MDCT findings) and intraoperative pathological findings. The NAC protocol consisted of four cycles of doxorubicin (50 mg m^{-2})/docetaxel (60 mg m^{-2}) with a 21-day cycle length (AT) or four cycles of fluorouracil (500 mg m^{-2})/epirubicin (100 mg m^{-2})/cyclophosphamide (500 mg m^{-2}) plus 12 weekly cycles of paclitaxel (80 mg m^{-2}) followed by surgery. The initial pathological confirmation of breast carcinoma was based on the findings of needle biopsy. All subjects gave informed consent to participate in the study, which was approved by the institutional review board of NCCH.

Preoperative imaging examinations

CT examinations were performed in the supine position using a helical CT scanner (single detector-row CT, X-vigor, Toshiba medical systems, Japan) between January and June 2000 and using an MDCT scanner (Aquilion, 4-rows and 16-rows ×0.5 mm, kV, mA, Toshiba) from July 2000. The first non-contrast-enhanced CT scan served as the baseline, with scanning performed from the cranial end of the sternum to the inframammary fold. Subsequently, an enhanced zoomed scan was obtained to visualize the entire breast, using a collimation of 5 mm and a pitch of 1 mm. A bolus of 100 ml of nonionic contrast material (300 mgI ml^{-1}) was injected intravenously at a rate of 3 ml s^{-1} via an antecubital vein on the side opposite the affected breast using an automated injector. Image acquisitions of early phase and late phase were started at 40 s and 180 s after the start of bolus injection of the contrast material. The reconstruction interval was 5 mm. Tumor shape was classified into two types: localized tumors (which were visualized as single lesions) and non-localized tumors (which included those with surrounding lesions, multiple lesions, or glandular spread) (Fig. 1). Tumor enhancement was classified into three types based on comparison between the early phase and the late phase: the wash-out pattern (early enhancement > late enhancement), the plateau pattern (early enhancement = late enhancement), and the persistent pattern (early enhancement < late enhancement).

All subjects also underwent both mammography and ultrasound examination before surgery. All ultrasound examinations were performed by experienced physicians who were aware of the results of physical examination. The findings of mammography and CT were retrospectively reviewed by two surgical oncologists working independently who were blinded to the findings of pathological examination. Tumor size measurements were obtained using each modality and compared with the size measured during pathological examination.

Histopathological examination

Pretreatment diagnosis was established by our pathologists on a core needle biopsy or a surgical resection. The diagnosis

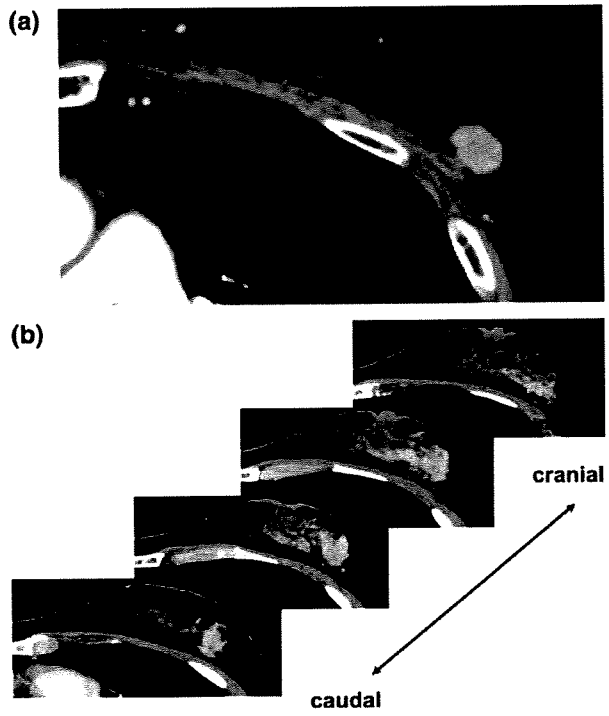

Fig. 1 Classification of invasive lobular carcinoma by CT imaging. **a** Localized tumor type, **b** non-localized tumor type

was based on tumor histology showing the absence of E-cadherin by immunohistological examination. Surgical specimens were sectioned at about 7–10 mm and maximum tumor diameters were measured on surgical specimens by pathologists. The pathological response of the primary tumor to NAC was classified according to the General Rules for Clinical and Pathological Recording of Breast Cancer [16]: grade 0 (no response observed), grade 1a (degenerative changes or severe degenerative changes in less than one-third of cancerous cells), grade 1b (severe degenerative changes in one-third to two-thirds of cancerous cells), grade 2 (degeneration of more than two-thirds of cancerous cells), and grade 3 (complete response, with no remaining cancerous cells). These slices were compared with the MDCT and the cranio-caudal view of the MMG and US.

Results

The median age of the 24 subjects with ILC was 52 years (range, 37 to 82 years). With regard to the clinical stage, 8 (42%) were stage I, 12 (50%) were stage IIA, 3 (13%) were stage IIB, and 1 (4%) was stage IIIA. Of the 24 subjects, 11 (46%) underwent total mastectomy and 13 (54%) underwent partial mastectomy. There was no case that had a changed operation method according to the results of intraoperative pathological diagnosis. The median tumor

Table 1 Clinicopathologic features of the study patients without NAC ($n = 24$)

Variable	Data
Age (years), median (range)	52 (37–82)
Clinical staging	
Stage I	8 (42%)
Stage IIA	12 (50%)
Stage IIB	3 (13%)
Stage IIIA	1 (4%)
Operation	
Total mastectomy	11 (46%)
Partial mastectomy	13 (54%)
Pathological tumor size (cm), median (range)	3.4 (1.1–8)

NAC neoadjuvant chemotherapy

diameter in the resected tissues was 3.4 cm (range 1.1–8 cm) (Table 1). There was no ILC lesion with wide LCIS, and so these diameters were obtained from the maximum measurement of invasive tumor cells extent. In addition, the median age of the 17 subjects with ILC who underwent NAC was 48 years (range 38 to 74 years). With regard to the clinical stage before the subjects underwent NAC, 7 (41%) were stage IIA, 5 (29%) were stage IIB, and 5 (29%) were stage IIIA. Of these 17 subjects, 3 (18%) underwent partial mastectomy, and 14 (82%) underwent total mastectomy. In addition, the median tumor diameter measured during pathological examination was 5.5 cm (range 1.9–13 cm). These diameters were the maximum extent of residual invasive tumor cells. Assessment of the pathological effects of NAC showed that one subject (6%) was grade 0, ten (59%) were grade 1a, five (29%) were grade 1b, and one (6%) was grade 2 (Table 2).

With regard to classification of the tumor shape by MDCT, localized-type tumors were observed in 9 subjects (37%) and non-localized-type tumors were observed in 15 subjects (63%) among the subjects with primary ILC, while localized-type tumors were observed in 3 subjects (18%) and non-localized-type tumors were observed in 13 subjects (76%) among the subjects with ILC who underwent NAC. With regard to tumor enhancement, 4 subjects (17%) showed the wash-out pattern, 9 (38%) showed the plateau pattern, and 11 (46%) showed the persistent pattern. This trend was more notable in subjects with ILC who underwent NAC. In most subjects, contrast enhancement was weak, and the plateau pattern (41%) or the persistent pattern (47%) was observed. It was impossible to assess the lesion in one subject with ILC who underwent NAC.

In the subjects with ILC who did not undergo NAC, the tumor diameter obtained at the time of preoperative evaluation and the tumor diameter measured during pathological examination were compared and evaluated (Fig. 2). The evaluation results showed that the tumor

Table 2 Clinicopathologic features of the study patients with NAC ($n = 17$)

Variable	Data
Age (years), median (range)	48 (38–74)
Clinical staging	
Stage IIA	7 (41%)
Stage IIB	5 (29%)
Stage IIIA	5 (29%)
Operation	
Total mastectomy	14 (82%)
Partial mastectomy	3 (18%)
Residural tumor size (cm), median (range)	5.5 (1.9–13)
Pathlogical response of NAC	
Grade 0	1 (6%)
Grade 1a	10 (59%)
Grade 1b	5 (29%)
Grade 2	1 (6%)
Grade 3	0 (0%)

NAC neoadjuvant chemotherapy

diameter was underestimated (smaller than the tumor diameter measured during pathological examination by 2 cm or more) in five subjects by MDCT, as compared with seven subjects (29%) each by mammography and ultrasound. In addition, the tumor diameter was overestimated (larger than the tumor diameter measured during pathological examination by 2 cm or more) in none of the subjects examined by any of the modalities.

The results obtained for the subjects with ILC who underwent NAC are shown in Fig. 3. Compared with the subjects with ILC who did not undergo NAC, it was extremely difficult to determine the tumor diameter in the preoperative evaluation. It was particularly difficult to measure the tumor diameter by ultrasound in many subjects. In addition, with ultrasound, it was possible to depict the residual tumors to some degree, but it was difficult to measure the residual tumor diameter. CT examination also showed the smallest number of subjects in which the error between the tumor diameter obtained by preoperative evaluation and the tumor diameter measured during pathological examination was 2 cm or more.

Tables 3 and 4 shows the diagnostic accuracy, underestimation rates, and overestimation rates for tumor diameter, based on the assumption that when the error between the tumor diameter obtained by preoperative evaluation and the tumor diameter measured during pathological examination was 2 cm or less, the tumor diameter was accurately determined. The diagnostic accuracy results for mammography, ultrasound, and MDCT were 53, 48, and 71%, respectively, in the subjects with ILC who underwent NAC. Compared with the subjects with ILC who did not undergo NAC, the diagnostic accuracy was found to be lower for all modalities, indicating that it is very difficult to evaluate the extent of ILC after NAC.

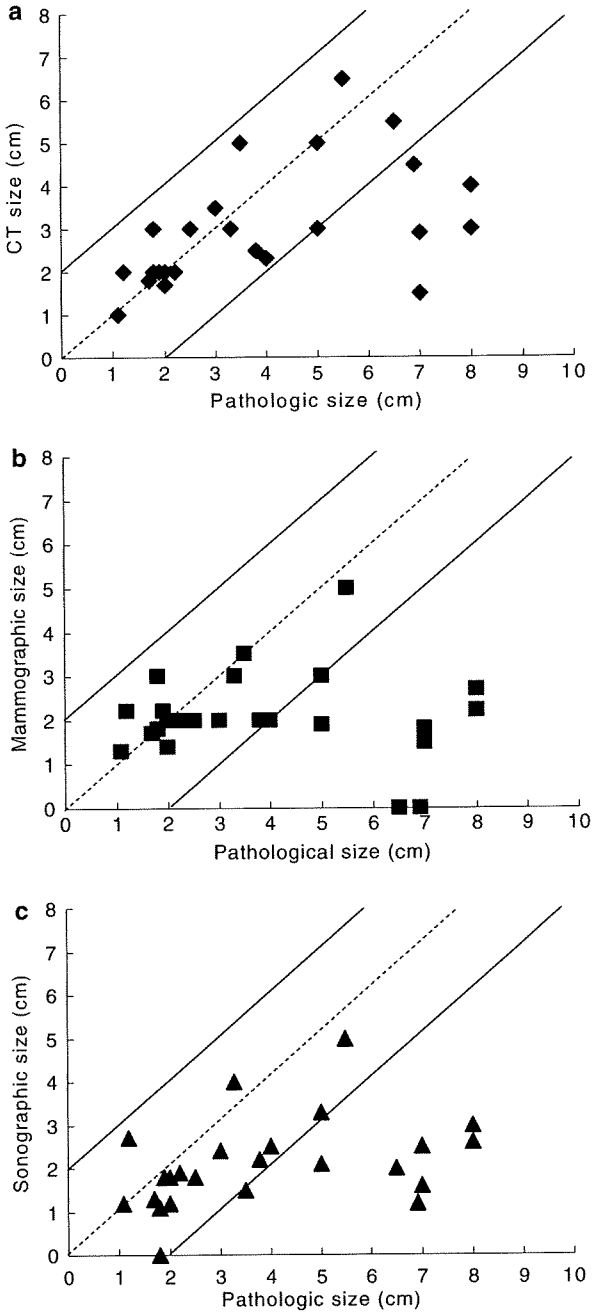

Fig. 2 Correlation between the MDCT, mammographic and sonographic sizes and pathological measurements in 24 ILC patients without NAC. **a** Correlation between MDCT sizes and pathological measurements, **b** correlation between mammographic sizes and pathological measurements, **c** correlation between sonographic sizes and pathological measurements

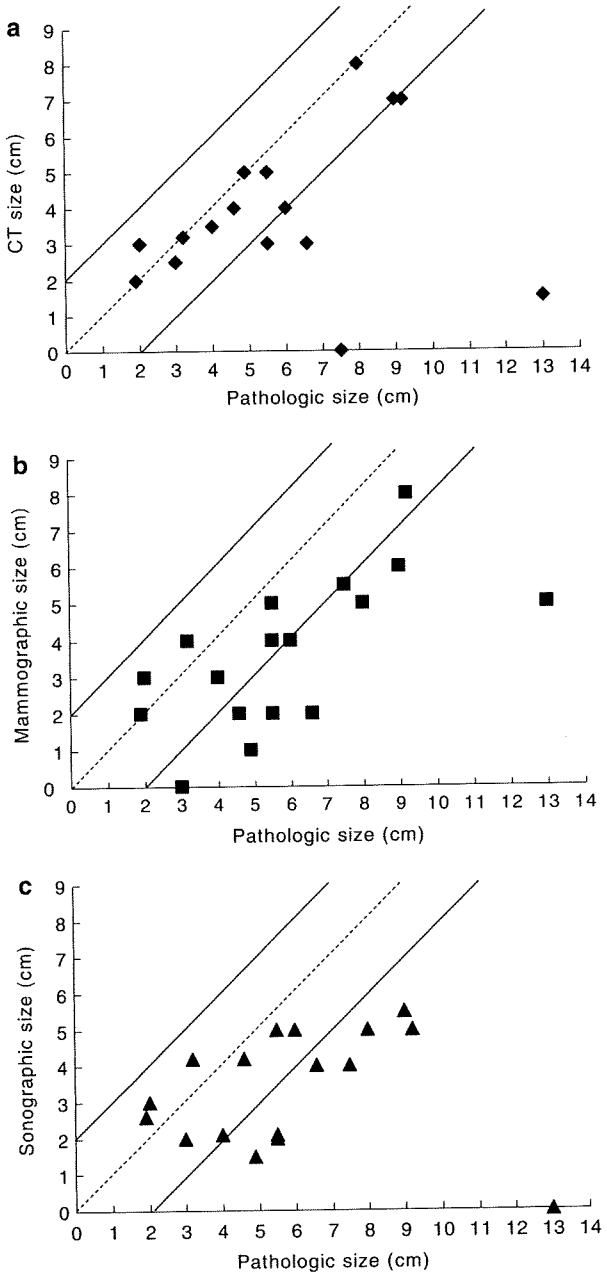

Fig. 3 Correlation between the MDCT, mammographic and sonographic sizes and pathological measurements in ILC patients with NAC. **a** Correlation between MDCT sizes and pathological measurements, **b** correlation between mammographic sizes and pathological measurements, **c** correlation between sonographic sizes and pathological measurements

Discussion

The results of the present study have shown that CT is more useful than mammography or ultrasound in determining the extent of ILC before surgery. In this study, since a safety margin of 2 cm was required when partial mastectomy was performed, it was determined that cases in which the measurement error was 2 cm or less could be accurately evaluated. The evaluation results for the subjects with ILC who did not undergo NAC showed that the diagnostic accuracy of MDCT was 79%, as compared with 71% for either mammography or ultrasound, indicating that the diagnostic accuracy of CT is higher than that of mammography or ultrasound. In addition, the tumor diameter obtained by preoperative evaluation was smaller than the tumor diameter measured during pathological examination in all subjects in which the measurement error was more than 2 cm.

Table 3 Classification of MDCT features in patients with ILC

Variable	ILC without NAC (n = 24)	ILC with NAC (n = 17)
Tumor shape		
Localized tumor type	9 (37%)	3 (18%)
Non-localized tumor type	15 (63%)	13 (76%)
Tumor enhancement		
Wash out pattern (early > late)	4 (17%)	1 (6%)
Plateau pattern (early = late)	9 (38%)	7 (41%)
Persistent pattern (early < late)	11 (46%)	8 (47%)

ILC invasive lobular carcinoma, *NAC* neoadjuvant chemotherapy

Other studies have reported that the extent of tumor tends to be underestimated [1, 2, 4, 9], especially by mammography and ultrasound, but CE-CT is more accurate than mammography and ultrasound. It is considered that these characteristics are very important in determining the extent of ILC. In fact, it is difficult to assess the extent of ILC, and the actual extent of ILC is larger than the evaluation result in most cases. Although the extent of ILC can be more precisely determined by CT, careful assessment is needed to avoid underestimation.

CT findings showed that ILC of the localized tumor type was relatively small, but ILC spreads diffusely into surrounding areas in many cases, and multiple lesions are observed in some cases. In addition, contrast enhancement of the tumor is relatively weak, and the good enhancement that is usually observed in the early enhancement phase in invasive intraductal carcinoma was not observed in many subjects.

On the other hand, gradual enhancement continuing to the late-enhancement phase, which is mainly observed in mastopathy or benign tumors, was seen in many subjects. It is therefore very important to differentiate between ILC and benign tumors in the diagnosis of ILC. It is also considered to be more difficult to precisely determine the extent of ILC as compared with invasive ductal carcinoma due to the lower percentage of localized tumors in addition to the weak contrast enhancement, which makes it difficult

Table 4 Accuracy of each modality for the detection of ILC

	ILC without NAC ($n = 24$)			ILC with NAC ($n = 17$)		
	Accuracy (%)	Underestimated (%)	Overestimated (%)	Accuracy (%)	Underestimated (%)	Overestimated (%)
Mammography	71	29	0	53	47	0
Ultrasound	71	29	0	48	52	0
MDCT	79	21	0	71	29	0

ILC invasive lobular carcinoma, *NAC* neoadjuvant chemotherapy, *MDCT* multidetector-row computed tomography

to evaluate ILC. It is therefore considered that these factors are involved in the observation that the tumor diameter obtained by preoperative evaluation using all modalities was smaller than the tumor diameter measured during pathological examination in many subjects as described above. In clinically, there are enhancement lesions that cannot be diagnosed clearly. This study demonstrated that if the main lesion was diagnosed as ILC before the operation, preoperative CT examination was useful, and these suspicious enhancement areas should be treated more carefully. Pathologically, ILC is characterized by the finding that some tumor cells lack the cell attachment factor E-cadherin and infiltrate the interstitial tissues at the cellular level [17, 18]. As a result, there are fewer new blood vessels and large amounts of interstitial tissue within the tumor, resulting in a low tumor cell density. This is considered to be the factor responsible for the fact that it is difficult to determine the extent of tumors with weak contrast enhancement.

In parallel with advances in antitumor agents, NAC, which has been used for regional advanced breast cancer, has also recently been employed for the treatment of breast cancers with a relatively small diameter before surgery. The objective of NAC is to reduce the size of the tumor and thus minimize the amount of breast tissue that must be resected. In other words, in patients who may be candidates for total mastectomy, NAC is performed to reduce the size of the tumor and permit the tumor to be completely resected, thus permitting breast-conserving therapy to be employed. Since it has been reported that obtaining a complete response (pCR) by NAC leads to an improved prognosis [19, 20], NAC is employed for small tumors to achieve pCR at many institutions. However, given this trend, many new problems have been recognized. One problem is that it is very difficult to assess the extent of residual tumor before surgery because tumors that have been substantially reduced by NAC cannot be clearly depicted. If the extent of residual tumor cannot be precisely assessed, not only may it be necessary to perform additional resection several times, but tumor cells may also remain in the remaining breast tissues even if no tumor cells are observed at the incision line if the tumor shows a mosaic-like pattern. In the subjects with ILC in the present study, it was difficult to assess the extent of the tumor even in the subjects who did not undergo NAC. In a number of studies, it has been reported that NAC is not suitable for ILC because it is difficult to assess the extent of residual tumor or to perform pathological diagnosis and because antitumor agents are less effective against ILC than invasive ductal carcinoma [9, 21, 22]. Considering these findings, it is considered that further evaluation is required.

As Berrington et al. [23] pointed out that the exposure dose by diagnostic X ray was the biggest among the 15 countries examined, we have to pay attention on the exposure dose carefully. For 16-row MDCT, which is used for routine examinations at our institution, regions including the axillary lymph nodes are included in the scan range. The exposure dose was 26 mSv for scanning in the non-contrast phase, the early-enhancement phase (40s), and the late-enhancement phase (3 min). This dose is about 13 times the exposure for mammography. However, CT was performed in a supine position similar to the operative position, so we can correctly evaluate the design of resection for breast-conserving therapy. There are helical CT scanners in many Japanese medium and small hospitals. Therefore, we can use CT without circumstance. We should consider these risks and benefits when we use CT examination for diagnosis.

In the present study, it was found that CT was more useful than mammography or ultrasound in the subjects with ILC who underwent NAC. The diagnostic accuracy of CT was found to be much higher than that of mammography or ultrasound. At the present time, however, the characteristics of CT images as obtained in this study may not permit comprehensive evaluation. It is not always easy to obtain preoperative diagnosis of ILC. However, in order to perform surgery safely in patients with a preoperative diagnosis of ILC or suspicion of it, it is recommended that diagnosis be performed with great care, taking the characteristics of ILC in CT images into consideration. It is necessary to evaluate more numbers of ILC patients and prospective studies to demonstrate the efficacy of preoperative CT examination.

References

1. Uchiyama N, Miyakawa K, Moriyama N, Kumazaki T. Radiographic features of invasive lobular carcinoma of the breast. Radiat Med. 2001;19(1):19–25.
2. Hikino H, Okada N, Kodama K, Takeda H, Ozaki N, Nagaoka S, Kai T. Computed-tomographic features of invasive lobular carcinoma. Clin Imaging. 2005;29:383–8.
3. Kneeshaw PJ, Turnbull LW, Smith A, Drew PJ. Dynamic contrast enhanced magnetic resonance imaging aids the surgical management of invasive lobular breast cancer. Eur J Surg Oncol. 2003;29:32–7.
4. Berg WA, Gutierrez L, NessAiver MS, Carter WB, Bhargavan M, Lewis RS, Loffe OB. Diagnostic accuracy of mammography, clinical examination, US, and MR imaging in preoperative assessment of breast cancer. Radiology. 2004;233(3):830–49.
5. Schelfout K, Goethem MV, Kersschot E, Verslegers I, Biltjes I, Leyman P, Colpaert C, Thienpont L, Haute JVD, Gillardin JP, Tjalma W, Buytaert PH, Schepper AD. Preoperative breast MRI in patients with invasive lobular cancer. Eur Radiol. 2004;14:1209–16.
6. Akashi-Tanaka S, Fukutomi T, Watanabe T, Katsumata N, Nanasawa T, Matsuo K, Miyakawa K, Tsuda H. Accuracy of contrast-enhanced computed tomography in the prediction of residual breast cancer after neoadjuvant chemotherapy. Int J Cancer. 2001;96:66–73.
7. Akashi-Tanaka S, Fukutomi T, Sato N, Iwamoto E, Watanabe T, Katsumata N, Ando M, Miyakawa K, Hasegawa T. The use of contrast-enhanced computed tomography before neoadjuvant chemotherapy to identify patients likely to be treated safely with breast-conserving surgery. Ann Surg. 2004;239:238–43.
8. Denis F, Desbiez-Bourcier AV, Chapiron C, Arbion F, Body G, Brunereau L. Contrast enhanced magnetic resonance imaging underestimates residual disease following neoadjuvant docetaxel based chemotherapy for breast cancer. Eur J Surg Oncol. 2004;30(10):1069–76.
9. Schott AF, Roubidoux MA, Helvie MA, Hayes DF, Kleer CG, Newman LA, Pierce LJ, Griffith KA, Murray S, Hunt KA, Paramagul C, Baker LH. Clinical, radiologic assessments to predict breast cancer pathologic complete response to neoadjuvant chemotharapy. Breast Cancer Res Treat. 2005;92(3):231–8.
10. Yeh E, Slanetz P, Kopans DB, Rafferty E, Georgian-Smith D, Moy L, Halpern E. Prospective comparison of mammography, sonography MRI in patients undergoing neoadjuvant chemotherapy for palpable breast cancer. AJR Am J Roentgenol. 2005;184(3):868–7.
11. Londero V, Bazzocchi M, Del Frate C, Puglisi F, Di Loreto C, Francescutti G, Zuiani C. Locally advanced breast cancer: comparison of mammography, sonography MR imaging in evaluation of residual disease in women receiving neoadjuvant chemotherapy. Eur Radiol. 2004;14(8):1371–9.
12. Akazawa K, Tamaki Y, Taguchi T, Tanji Y, Miyoshi Y, Kim SJ, Ueda S, Yanagisawa T, Sato Y, Tamura S, Noguchi S. Preoperative evaluation of residual tumor extent by three-dimensional magnetic resonance imaging in breast cancer patients treated with neoadjuvant chemotherapy. Breast J. 2006;12(2):130–7.
13. Belli P, Costantini M, Malaspina C, Magistrelli A, Latorre G, Bonomo L. MRI accuracy in residual disease evaluation in breast cancer patients treated with neoadjuvant chemotherapy. Clin Radiol. 2006;61(11):946–53.
14. Peintinger F, Kuerer HM, Anderson K, Boughey JC, Meric-Bernstam F, Singletary SE, Hunt KK, Whitman GJ, Stephens T, Buzdar AU, Green MC, Symmans WF. Accuracy of the combination of mammography and sonography in predicting tumor response in breast cancer patients after neoadjuvant chemotherapy. Ann Surg Oncol. 2006;13(11):1443–9.
15. Chagpar AB, Middleton LP, Sahin AA, Dempsey P, Buzdar AU, Mirza AN, Ames FC, Babiera GV, Feig BW, Hunt KK, Kuerer HM, Meric-Bernstam F, Ross MI, Singletary SE. Accuracy of physical examination, ultrasonography, and mammography in predicting residual pathologic tumor size in patients treated with neoadjuvant chemotherapy. Ann Surg. 2006;243(2):257–64.
16. The Japanese Breast Cancer Society. General rules for clinical and pathological recording of breast cancer. 15th ed. Tokyo: Kanehara; 2004.
17. Margenthaler JA, Duke D, Monsees BS, Barton PT, Clark C, Dietz JR. Correlation between core biopsy and excisional biopsy in breast high-risk lesions. Am J Surg. 2006;192:534–7.
18. Doyle EM, Banville N, Quinn CM, Flanagan F, O'Doherty A, Hill AD, Kerin MJ, Fitzpatrick P, Kennedy M. Radial scars/complex sclerosing lesions and malignancy in a screening programme: incidence and histological features revisited. Histopathology. 2007;50:607–14.
19. Fisher B, Bryant J, Wolmark N, Mamounas E, Brown A, Fisher ER, Wickerham DL, Begovic M, DeCillis A, Robidoux A, Margolese RG, Crus Jr AB, Hoehn JL, Lees AW, Dimitrov NV, Bear HD. Effect of preoperative chemotherapy on the outcome of women with operable breast cancer. J Clin Oncol. 1998;16(8):2672–85.
20. Kuerer HM, Newman LA, Smith TL, Ames FC, Hunt KK, Dhingra K, Theriault RL, Singh G, Binkley SM, Sneige N, Buchholz TA, Ross MI, McNeese MD, Buzdar AU, Hortobagyi GN, Singletary SE. Clinical course of breast cancer patients with complete pathologic primary tumor and axillary lymph node response to doxorubicin-based neoadjuvant chemotherapy. J Clin Oncol. 1999;17(2):460–9.
21. Tubiana-Hulin M, Stevens D, Lasry S, Guinebretiere M, Bouita L, Cohen-Solal C, Cherel P, Rouesse J. Response to neoadjuvant chemotherapy in lobular and ductal breast carcinomas: a retrospective study on 860 patients from one institution. Ann Oncol. 2006;17:1228–33.
22. Cocquyt VF, Blondeel PN, Depypere HT, Praet MM, Scelfhout VR, Silvia OE, Hurler J, Serreyn RF, Daems KK, Van Belle SJ. Different response to preoperative chemotherapy for invasive lobular carcinoma and invasive ductal carcinoma. Eur J Surg Oncol. 2003;29(4):361–7.
23. Berrington de Gonzalez A, Darby S. Risk of cancer from diagnostic X-rays: estimates for the UK and 14 other countries. Lancet. 2004;363(9406):345–51.

Cancer Science
The official journal of the Japanese Cancer Association JCA

Tumor histology in lymph vessels and lymph nodes for the accurate prediction of outcome among breast cancer patients treated with neoadjuvant chemotherapy

Nobuko Tamura,[1,2,7] Takahiro Hasebe,[2,7] Nao Okada,[1] Takashi Houjoh,[1] Sadako Akashi-Tanaka,[1] Chikako Shimizu,[3] Tatsuhiro Shibata,[4] Yuko Sasajima,[5] Motoki Iwasaki[6] and Takayuki Kinoshita[1]

[1]Department of Breast Surgery, National Cancer Center Hospital, Chuo-ku, Tokyo; [2]Pathology Consultation Service, Clinical Trials and Practice Support Division, Center for Cancer Control and Information Services, National Cancer Center, Chuo-ku, Tokyo; [3]Division of Breast and Medical Oncology, National Cancer Center Hospital, Chuo-ku, Tokyo; [4]Cancer Genomics Project, National Cancer Center Research Institute, Chuo-ku, Tokyo; [5]Clinical Laboratory Division, National Cancer Center Hospital, Chuo-ku, Tokyo; [6]Epidemiology and Prevention Division, Research Center for Cancer Prevention and Screening, National Cancer Center, Chuo-ku, Tokyo, Japan

(Received May 11, 2009/Revised June 6, 2009/Accepted June 14, 2009/Online publication July 13, 2009)

The present study investigated fibrotic foci (FFs), the grading system for lymph vessel tumor emboli (LVTEs), and the histological characteristics of nodal metastatic tumors that were significantly associated with the outcomes of 115 patients with invasive ductal carcinoma (IDC) who had received neoadjuvant chemotherapy. We compared the outcome predictive power of FFs, the grading system for LVTEs, and the histological characteristics of metastatic tumors in lymph nodes with the well-known clinicopathological characteristics of tumor recurrence and tumor-related death in multivariate analyses. The presence of FFs, as assessed by a biopsy performed before neoadjuvant chemotherapy, significantly increased the hazard rates (HRs) for tumor-related death in all the cases and in cases with nodal metastasis. The grading system for LVTEs, which was assessed using surgical specimens obtained after neoadjuvant chemotherapy, was significantly associated with increasing hazard rates (HRs) for tumor recurrence and tumor-related death in all the cases and in cases with nodal metastasis. Moderate to severe stroma in nodal metastatic tumors and five or more mitotic figures in nodal metastatic tumors were significantly associated with elevated HRs for tumor recurrence and tumor-related death among all the cases. These results indicated that FFs, the grading system for LVTEs, and the histological characteristics of tumor cells in lymph nodes play important roles in predicting the tumor progression of IDCs of the breast in patients treated with neoadjuvant chemotherapy. (*Cancer Sci* 2009; 100: 1823–1833)

Traditionally, neoadjuvant chemotherapy has been used for the treatment of locally advanced or inoperable breast cancer.[1,2] More recently, neoadjuvant chemotherapy has been used for the treatment of patients with smaller tumors that would have previously been considered operable at the patient's initial presentation.[3] The purpose of neoadjuvant chemotherapy is to reduce the size of the primary tumor in the breast, so as to facilitate breast conservation surgery, and also to abolish or reduce the disease burden associated with micro-metastatic disease with the intention of prolonging the patient's overall survival.

Gene or protein expression profiles have recently been reported to be significant predictors of the outcome of patients receiving neoadjuvant chemotherapy.[4–6] However, identifying histological predictors of prognosis is very important because histopathological examinations of invasive ductal carcinomas (IDCs) can be routinely performed at any hospital and also are a very useful method for following IDC patients who received neoadjuvant chemotherapy clinically. Clinicopathological factors including age, residual invasive tumor size, histologic grade of the primary invasive tumors, axillary node status, and pathological response have been reported to be good predictors of prognosis among patients with IDC who have received neoadjuvant chemotherapy,[7–10] and we recently demonstrated that a grading system for lymph vessel tumor emboli (LVTEs) and the histological characteristics of tumor cells in lymph nodes are very important histological predictors of prognosis among IDC patients who did not receive neoadjuvant therapy.[11,12] These findings strongly suggest that a grading system for LVTEs or the histological characteristics of tumor cells in lymph node might also be very important histological predictors of prognosis among IDC patients who received neoadjuvant chemotherapy.

The purpose of this study was to investigate the histological characteristics of primary invasive tumors, the grading system for LVTEs, and the histological characteristics of nodal metastatic tumors that were significantly associated with the outcomes of IDC patients who received neoadjuvant chemotherapy. We found that the presence of fibrotic foci (FFs), as assessed using biopsy materials obtained before neoadjuvant chemotherapy; the grading system for LVTEs, as assessed using surgical specimens obtained after neoadjuvant chemotherapy; and several histological characteristics of tumor cells in lymph nodes, as assessed using surgical specimens obtained after neoadjuvant chemotherapy, had significant effects on outcome among IDC patients who received neoadjuvant chemotherapy.

Materials and Methods

Patients. The subjects of this study comprised 115 consecutive patients with IDC of the breast who had been surgically treated at the National Cancer Center Hospital between January 1997 and December 2002. The IDCs were diagnosed preoperatively by aspiration cytology, mammography, or ultrasonography. Clinical information was obtained from the patients' medical records after a complete histological examination of all the IDCs. All the patients were Japanese women, ranging in age from 30 to 71 years (median, 50 years). All the patients had a solitary lesion; 49 patients were premenopausal, and 57 were postmenopausal. A partial mastectomy had been performed in 14 patients, and a

[7]To whom correspondence should be addressed.
E-mail: nobtamur@ncc.go.jp or thasebe@ncc.go.jp

doi: 10.1111/j.1349-7006.2009.01264.x

Table 1. Criteria used in the grading systems for lymph vessel tumor emboli in invasive ductal carcinoma (IDC)

Grading system for lymph vessel tumor emboli according to the number of mitotic and apoptotic figures in tumor cells of lymph vessel tumor emboli		
Grade 0	IDCs with no lymph vessel tumor emboli	
Grades 1, 2, and 3	IDCs with one or more lymph vessel tumor emboli	
	No. of mitotic figures	No. of apoptotic figures
Grade 1	Low-proliferative type	
1a	0	0
1b	0	>0
1c	>0	0
Grade 2	Intermediate-proliferative type	
2a	1 to 4	>0
2b	>0	1 to 6
Grade 3	High-proliferative type	
3a	>4	>6

modified radical mastectomy had been performed in 101. A level I and II axillary lymph node dissection had been performed in all the patients, and a level III axillary lymph node dissection had been performed in some of the IDC patients.

Of the 115 patients, 17 (12%) had only residual ductal carcinoma *in situ*, while 98 (88%) patients had residual IDC; none of the patients exhibited a pathological complete response (no tumor) to neoadjuvant chemotherapy. All the neoadjuvant chemotherapy regimens were anthracycline-based with or without taxane. No cases of inflammatory breast cancer were encountered in this series. All the tumors were classified according to the pathological International Union Against Cancer (UICC)-TNM (pTNM) classification.[13]

For the pathological examination, biopsy specimens obtained before neoadjuvant chemotherapy and surgically resected specimens obtained after neoadjuvant chemotherapy were fixed in 10% formalin and subsequently examined. The size and gross appearance of the surgically resected tumor specimens were recorded as the residual invasive tumor size. The tumor size of the surgically resected specimens was confirmed by comparison with the tumor size on histological slides; if more than one invasive focus was present, the size of the largest invasive focus was recorded as the residual invasive tumor size in this study.

Histological examination. Serial sections of the biopsy materials obtained before neoadjuvant chemotherapy, and serial sections of the tumor area in the surgically resected materials obtained after neoadjuvant chemotherapy were cut from paraffin blocks. One section of each biopsy or surgical specimen was stained with hematoxylin and eosin (H&E) and examined histologically to confirm the diagnosis, and another section was subjected to immunohistochemistry. The following eight histological features of the primary invasive tumors were evaluated in the biopsy materials obtained before neoadjuvant chemotherapy and the surgical materials obtained after neoadjuvant chemotherapy: (1) clinical invasive tumor size or residual invasive tumor size (≤20, >20 to ≤0, >50 mm); (2) histologic grade (1, 2, 3);[14] (3) tumor necrosis (absent, present);[15] (4) FF (absent, present) (Fig. 1a,b);[16,17] (5) blood vessel invasion (absent, present); (6) adipose tissue invasion (absent, present); and (7) skin invasion (absent, present). We also evaluated a grading system for LVTEs, as assessed using biopsy materials obtained before neoadjuvant chemotherapy and surgical materials obtained after neoadjuvant chemotherapy (Table 1, Fig. 1c,d).[11] Briefly, the number of tumor cell mitotic figures and the number of apoptotic figures in the lymph vessels were counted in 20 high-power fields of the surgical materials. In practice, for the surgical materials, we first examined all the slides of the IDCs containing both tumor areas and non-tumor areas to identify the LVTEs. Next, we selected the LVTEs, e.g. large LVTEs located far from the stroma–invasive tumor margin, and recorded the number of mitotic figures and the number of apoptotic figures in the tumor cells composing the LVTEs of the IDC. The mitotic and apoptotic figures were counted under a high-power field, and the largest number of mitotic figures and/or the largest number of apoptotic figures were recorded as the number of mitotic figures and apoptotic figures in the LVTEs of the IDC, respectively. The cumulative numbers of tumor cell mitotic figures and apoptotic figures in the LVTEs in all 20 high-power fields were not used. In IDCs containing a small number of LVTEs, the mitotic figures and apoptotic figures were counted in less than 20 high-power fields. For the biopsy materials, we examined the presence or absence of LVTE or LVTEs; when LVTE or LVTEs were observed in the biopsy material, an assessment similar to that described above was performed. We also evaluated the prognostic predictive power of the location of lymph vessel invasion,[18] the Fisher's neoadjuvant-chemotherapy-effect classification,[19,20] and the Japanese Breast Cancer Society (JBCS) neoadjuvant-chemotherapy-effect classification for surgical materials obtained after neoadjuvant chemotherapy.[21] Cases with non-invasive ductal carcinoma (NIDC) after neoadjuvant chemotherapy were classified as belonging to grade 3 of the JBCS neoadjuvant-chemotherapy effect classification.[21] None of the IDC cases exhibited the disappearance of all the tumor cells (invasive tumor cells and non-invasive tumor cells) after neoadjuvant chemotherapy in this series.

The following histological features of metastatic tumors in lymph nodes dissected at the time of surgery (after neoadjuvant chemotherapy) were examined:[12] (1) the maximum dimension of nodal metastatic tumors; (2) lymph nodes with extra-nodal invasion (absent, present); (3) extra-nodal blood vessel tumor emboli (absent, present); (4) number of mitotic figures in tumors in the lymph node (≤5, >5); (5) histologic grade of tumors in the lymph node (1, 2, 3); and (6) grade of stromal fibrosis of tumors in the lymph node (none, mild, moderate, severe) (Fig. 1e,f). Extra-nodal invasion was defined as the extension of tumor cells through the capsule of at least one lymph node into the perinodal adipose tissue. Nuclear atypia, structural atypia, and the number of mitotic figures were evaluated in the same manner as for the primary invasive tumors. The presence of metastases in the lymph nodes was evaluated using single sections of each node or half of each node stained with H&E.

Immunohistochemistry. Immunohistochemical staining for estrogen receptors (ERs), progesterone receptors (PRs), and HER2 products was performed using an autoimmunostainer (Optimax Plus; BioGenex, San Ramon, CA, USA). The antigen retrieval device of the Optimax Plus was autoclaved, and each specimen was immersed in citrate buffer and incubated at 121°C for 10 min. Immunoperoxidase staining was performed using a labeled streptavidin biotin staining kit (BioGenex) according to the manufacturer's instructions. The antibodies used were an

doi: 10.1111/j.1349-7006.2009.01264.x

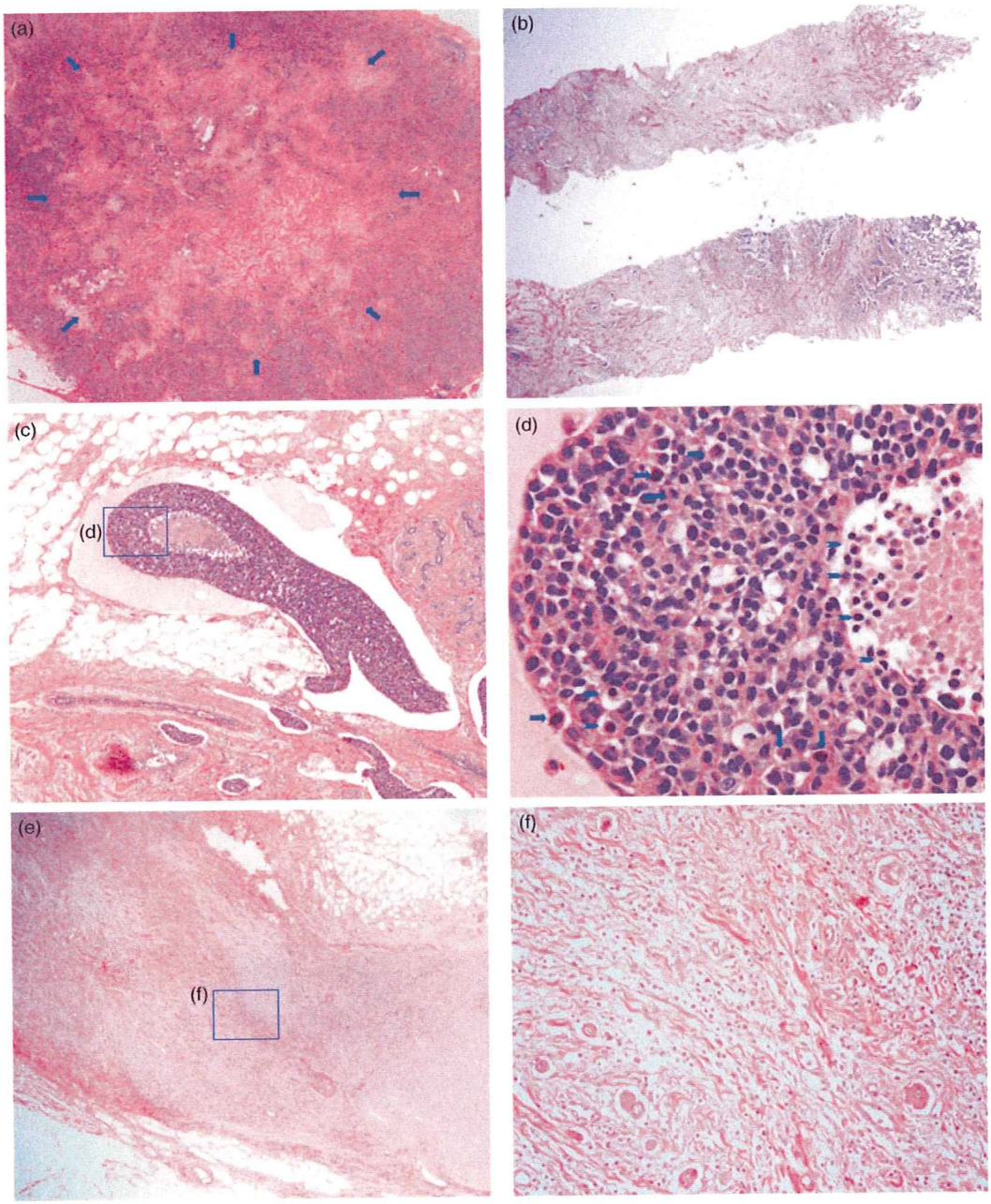

Fig. 1. Histological characteristics of fibrotic foci (FFs), lymph vessel tumor emboli, and nodal metastatic tumors. (a) An FF measuring 8.4 × 6.2 mm is visible within the tumor (arrows) in a surgical specimen. The FF has the appearance of a scar-like feature, and it is surrounded by invasive ductal carcinoma cells. The FF area consists of fibroblasts and collagen fibers arranged in a storiform pattern with tumor cell nests. (b) A core-needle biopsy specimen shows an FF consisting of fibroblasts and collagen fibers in a storiform arrangement intermingled with invasive tumor cells (fibrosis grade 3). (c) One large lymph vessel tumor embolus and five lymph vessel tumor emboli are shown. A necrotic tumor focus is visible in the large lymph vessel tumor embolus. (d) Several apoptotic bodies and apoptotic tumor cells are visible (arrowheads), and six mitotic tumor cells (arrows) can be seen in the lymph vessel tumor embolus. The apoptotic bodies are small, variously shaped pyknotic bodies that resemble sesame seeds, and the apoptotic tumor cells were identified as tumor cells containing eosinophilic or amphophilic cytoplasm and irregularly shaped pyknotic nuclei. (e) Metastatic tumor in the lymph node exhibiting dense stromal fibrosis. (f) Tumor cells with light eosinophilic cytoplasm and irregularly shaped nuclei exhibiting scattered growth in dense fibrous stroma of a metastatic tumor in a lymph node.

anti-ER mouse monoclonal antibody (mAb), ER88 (BioGenex); an anti-PR mAb, PR88 (BioGenex); and an anti-HER2 mAb, CB11 (BioGnex). ER88, PR88, and CB11 were already diluted. After immunostaining, the sections were counterstained with hematoxylin. Sections of IDCs positive for ER, PR, and HER2 were used each time as a positive control. As a negative control, the primary antibody was replaced with normal mouse immunoglobin. An IDC with nuclear staining for ER or PR in 10% or more of its tumor cells was assessed as ER-positive or PR-positive. The HER2 status of the tumor cells was semi-quantitatively scored on a 0 to 3 scale according to the level of HER2 protein expression.[22]

One author (N.T.) assessed all the characteristics of the primary tumors, the tumors in the lymph vessels, and the nodal